




Cite this: *Anal. Methods*, 2022, **14**, 4555

# Process integrated biosensors for real-time monitoring of antibodies for automated affinity purification†

Thuy Tran,<sup>a</sup> Erik Martinsson,<sup>b</sup> Robert Gustavsson,<sup>c</sup> Otto Tronarp,<sup>d</sup> Mats Nilsson,<sup>e</sup> Kristoffer Rudenholm Hansson,<sup>e</sup> Ingemar Lundström,<sup>f</sup> Carl-Fredrik Mandenius<sup>c</sup> and Daniel Aili  <sup>\*a</sup>

Therapeutic monoclonal antibodies (mAbs) provide new means for treatments of a wide range of diseases and comprise a large fraction of all new approved drugs. Production of mAbs is expensive compared to conventional drug production, primarily due to the complex processes involved. The affinity purification step is dominating the cost of goods in mAb manufacturing. Process intensification and automation could reduce costs, but the lack of real-time process analytical technologies (PAT) complicates this development. We show a specific and robust fiber optical localized surface plasmon resonance (LSPR) sensor technology that is optimized for in-line product detection in the effluent in affinity capture steps. The sensor system comprises a flow cell and a replaceable sensor chip functionalized with biorecognition elements for specific analyte detection. The high selectivity of the sensor enable detection of mAbs in complex sample matrices at concentrations below 2.5  $\mu\text{g mL}^{-1}$ . In place regeneration of the sensor chips allowed for continuous monitoring of multiple consecutive chromatographic separation cycles. Excellent performance was obtained at different purification scales with flow rates up to 200  $\text{mL min}^{-1}$ . This sensor technology facilitates efficient column loading, optimization, and control of chromatography systems, which can pave the way for continuous operation and automation of protein purification steps.

Received 26th September 2022  
Accepted 21st October 2022

DOI: 10.1039/d2ay01567f

[rsc.li/methods](https://rsc.li/methods)

## 1. Introduction

The first therapeutic monoclonal antibody (mAb) was approved by the United States Food and Drug Administration (US FDA) in 1986.<sup>1</sup> Since then, mAbs have become major class of new drugs for treatment of a wide range of diseases with significant market growth.<sup>2</sup> Although the drugs are becoming increasingly more sophisticated, the production is still typically conducted as a series of discrete unit operations with limited automation.<sup>3</sup> Affinity chromatography using resins with Protein A or similar variants is currently the dominating method of choice in mAb bioproduction to isolate,

concentrate, and stabilize the product.<sup>4–7</sup> Due to the high selectivity and stability of the resins, product purities of more than 95% can be achieved, and resins can be reused over many cycles.<sup>8</sup> Despite the excellent performance, Protein A capture is the most expensive step in the downstream purification procedure, mainly because of the high cost of recombinant Protein A resins.<sup>9</sup> Consequently, there has been significant efforts to reduce the cost of this unit operation by, for example, developing novel synthetic mAb ligands or affinity membrane filtration strategies.<sup>10</sup> Another direction is to combine the single-column purification set-up into a sequential multi-column system which allows the product breakthrough of one column to be redirected into another column.<sup>11</sup> Continuous multi-column protein A chromatography has been reported to increase the utilization of column capacity while keeping sample loss at a minimum level.<sup>11–13</sup> However, to control the loading phase and timely divert unbound mAbs from the first to the second column in the series requires reliable real-time detection of product breakthrough, which is currently very challenging.

Real-time detection of products in the effluent during loading becomes even more indispensable in a continuous integrated antibody production process. In a continuous approach,<sup>14,15</sup> mAbs are produced in a perfusion bioreactor,

<sup>a</sup>Laboratory of Molecular Materials, Division of Biophysics and Bioengineering, Department of Physics, Chemistry and Biology, Linköping University, Linköping 581 83, Sweden. E-mail: [daniel.aili@liu.se](mailto:daniel.aili@liu.se)

<sup>b</sup>ArgusEye AB, Spannmålgatan 55, Linköping 583 36, Sweden

<sup>c</sup>Biotechnology, Division of Biophysics and Bioengineering, Department of Physics, Chemistry and Biology, Linköping University, Linköping 581 83, Sweden

<sup>d</sup>Wolfram MathCore AB, Teknikringen 1E, Linköping 583 30, Sweden

<sup>e</sup>BioInvent International AB, Ideon Science Park, Lund 223 70, Sweden

<sup>f</sup>Sensor and Actuator Systems, Department of Physics, Chemistry and Biology, Linköping University, Linköping 581 83, Sweden

† Electronic supplementary information (ESI) available. See DOI: <https://doi.org/10.1039/d2ay01567f>



captured directly on Protein A columns after passing a cell removal device, and subsequently processed in other downstream process steps without any hold times or interruptions in between the different unit operations. In a traditional scenario using fed-batch reactors, loaded mass can generally be estimated by taking into account column capacity and pre-determined product titers. In the continuous production approach, titers in the cell-free harvest vary during the loading phase and in different purification cycles. Real-time titer measurements must therefore be carried out. However, this type of analysis remains a major challenge with current standard methodologies such as Protein A/G high performance liquid chromatography (HPLC) and enzyme linked immunosorbent assays (ELISA).<sup>16–18</sup> Both methods are time-consuming and typically carried out in an off-line setting. In addition, the operating conditions of the purification process leads to deterioration of the column performance over time. It has been shown that the initial mAb binding capacity of Protein A columns can decrease up to 40% after 100 repeated purification cycles.<sup>19–21</sup> Therefore, loaded mass calculated based on initial maximum capacity becomes less accurate already after a few cycles. Real-time detection of products in the breakthrough fluid circumvents the need to know column capacity and product titer during loading and would facilitate development of continuous integrated production approaches.

Significant effort has been made to develop in-line real-time process analytical technologies (PAT) to monitor and control continuous multi-column chromatography steps and to intensify production. Ultra-violet (UV) detectors are widely used to monitor breakthrough curves based on the absorption of UV light by proteins. By monitoring the difference in signal ( $\Delta UV$ ) between two UV cells positioned at the column inlet and outlet, sample diversion to the subsequent column can be initiated at a certain  $\Delta UV$  value corresponding to a desired breakthrough percentage.<sup>22</sup> Measuring  $\Delta UV$  at multiple wavelengths to reduce signal variations<sup>23</sup> or using variable pathlengths of the UV cells to avoid detector saturation<sup>24</sup> have been shown to improve detection of breakthrough levels. However, the low UV signal compared to background absorbance caused by non-product related impurities and media components in the effluent significantly complicates breakthrough detection. In addition, the background signals vary substantially depending on cell culture feeds, which is difficult to compensate for by varying the UV cell path length.

Here we show a novel approach for in-line real-time detection of antibodies (IgG) and domain antibodies (dAbs) in the effluent in affinity capture steps using a fiber optical localized surface plasmon resonance (LSPR) sensor system. The LSPR sensor flow cell was mounted at the outlet of the affinity column and before the UV detector in an ÄKTA purification system (Fig. 1). A replaceable sensor chip, modified with gold nanostructures, was inserted into the flow cell connected to a light source and spectrometer using an optical fiber. The surface of the sensor chip was functionalized with Protein A or Protein L for selective binding of IgG or dAbs, respectively. The working principle of the LSPR technique was described in a previous report.<sup>25</sup> Briefly, the binding of the target protein to the

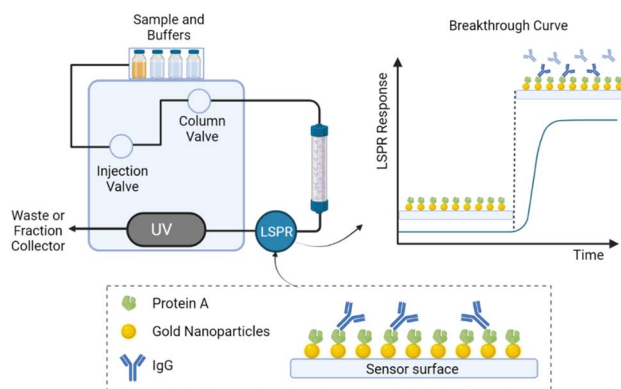


**Fig. 1** Illustration of in-line detection of IgG during the loading phase in a purification set-up using a Protein A column to capture IgG from cell culture supernatants. An LSPR flow cell was connected after the affinity column to monitor the presence of IgG in the effluent during sample loading. The LSPR flow cell contains a replaceable sensor chip with gold nanostructures functionalized with Protein A. Selective binding of IgG to the surface when the IgG breaks through the column gives rise to a plasmon peak shift, recorded as an LSPR response and shown as a breakthrough curve.

recognition element (Protein A or Protein L) on the sensor chip induces a local refractive index change in the vicinity of the nanostructures, which alters the optical resonance conditions and hence the position of the LSPR band. The resulting optical shift of the LSPR band ( $\Delta\lambda$ ) is recorded with picometer (pm) resolution in real-time. Compared to other approaches recently developed, such as, quartz crystal microbalance (QCM) sensors functionalized with Protein A for selective in-line detection of antibodies in the effluent,<sup>26</sup> and near-infrared (NIR) spectroscopy combined with computer-based algorithms to measure feed titers in real-time,<sup>27</sup> LSPR<sup>25</sup> is less sensitive to temperature changes, variation in sample composition, and vibrations and do not require any advanced data analysis to extract product concentrations.

The LSPR sensor approach was benchmarked against UV for detection of column breakthrough using cell culture supernatants and was found to drastically outperform UV-based methods regarding sensitivity and specificity. The UV detector was rapidly saturated due to sample background effects, making detection of breakthrough very challenging. In contrast, the LSPR sensor was capable of detecting breakthroughs or leakage caused by column aging at extremely low IgG concentrations, down to  $2 \mu\text{g mL}^{-1}$ , in effluents from samples with complex compositions. The sensor strategy was evaluated using different analytes and purification scales and with several cycles of purification, demonstrating high robustness of the sensor system and possibilities to regenerate the sensor in-line for continuous reuse of the sensor chips. We show that the developed in-line LSPR sensor approach provides a robust and reliable tool for real-time control of the loading phase in a multi-column purification system and for detection of column aging over multiple purification cycles, thus representing an enabling technology for continuous integrated bioproduction.



## 2. Experimental

### 2.1. Reagents and materials

Protein A and PBS tablets were obtained from Medicago AB (Uppsala, Sweden). *N*-Ethyl-*N'*-(3-dimethylaminopropyl)carbodiimide (EDC), *N*-hydroxysuccinimide (NHS), 4-morpholineethanesulfonic acid (MES), ethanolamine, sodium citrate dihydrate, citric acid and glycine were from Sigma-Aldrich (St. Louis, MO, USA). IgG and domain antibody (dAb) cell culture supernatants with concentrations of 1.1 mg mL<sup>-1</sup> and 1.4 mg mL<sup>-1</sup>, respectively, were provided by Testa Center (Uppsala, Sweden). Purified human IgG1 monomers (3.6 mg mL<sup>-1</sup>, 99% purity) were provided by BioInvent International AB (Lund, Sweden). LSPR sensor chips were obtained from ArgusEye AB (Linköping, Sweden).

### 2.2. Sensor chips functionalization

Carboxylate-functionalized sensor chips were activated by a 45 min incubation with 20 µL of 0.4 M EDC and 0.1 M NHS. The chips were thereafter rinsed using Milli-Q water (18.2 MΩ cm<sup>-1</sup>) and 20 µL of 0.5 mg mL<sup>-1</sup> protein A or protein L solutions prepared in MES buffer pH 6.0 was added to the surface. The coupling reaction was carried out for two hours, followed by a deactivation step using 20 µL of 1 M ethanolamine (pH 8.5) for 30 min. The sensor chips were rinsed using Milli-Q water and stored in PBS buffer before being inserted into the LSPR sensor system.

### 2.3. CHO cell cultivation

A recombinant CHO cell line (CHOK-1 derivative cell line) producing human IgG was provided from Cobra Biologics Ltd (Newcastle, UK). The cells were cultured in a spinner flask in fed-batch mode at 37 °C in a humidified atmosphere containing 7.5% CO<sub>2</sub>. HyClone Actipro™ medium supplemented with 3% GlutaMAX™ (100×) was used as culture media. On day three of culture, a daily feed of 2% HyClone Cell Boost™ 7a and 0.2% HyClone Cell Boost™ 7b of the culture volume was added. After 10 days the culture was centrifuged (200g, 5 min) and the supernatant was filtered through a 0.2 µm filter before affinity chromatography. The IgG concentration was determined by at-line LSPR. A stock IgG1 solution (3.6 mg mL<sup>-1</sup>) was spiked into the cell supernatant to obtain a higher total concentration of 1.5 mg mL<sup>-1</sup>.

### 2.4. Affinity purification and in-line LSPR measurements

The LSPR sensor system was evaluated using different ÄKTA systems as described in more detail below, including ÄKTA Pure 25, ÄKTA Purifier and ÄKTA Pilot. LSPR measurements were performed using a fiber optical sensor system provided by ArgusEye AB (Linköping, Sweden), comprising a flow cell, a white light source and a spectrophotometer. The LSPR sensor flow cell was connected to the column outlet before the UV cell in the ÄKTA systems. LSPR signals were recorded in real-time using the ArgusEye software.

#### 2.4.1. In-line measurements of IgG in cell supernatants.

Samples from cell cultures with IgG concentrations of 0.07 mg mL<sup>-1</sup> and 1.5 mg mL<sup>-1</sup> were purified on an ÄKTA Pure 25 system, using a HiTrap MabSelect SuRe column 1 mL, at flow rate of 1 mL min<sup>-1</sup>. A Protein A sensor chip was used. Ten column volumes (CV) of PBS were used to equilibrate the column. After loading the sample until the product breakthrough was seen, the column was washed using about 20 CV of PBS. Elution was performed using 10 CV of citrate 50 mM, pH 2.5.

**2.4.2. Multicycle purification.** Cell culture supernatant with an IgG concentration of 1.1 mg mL<sup>-1</sup> was purified on an ÄKTA Pure 25 system with a MabSelect Prisma 1 mL column at a flow rate of 1 mL min<sup>-1</sup>. A Protein A sensor chip was used. 20 mM sodium phosphate containing 150 mM NaCl, pH 7.2 was used for column equilibration (5 CV) and column washing (12 CV) after sample loading (47 CV). Elution was done using 50 mM citrate, pH 3.5 (10 CV). To regenerate both the affinity column and the LSPR sensor chips, a stripping step using 50 mM citrate, pH 2.5 (7 CV) was used after the elution phase. In this experiment Open Platform Communication Data Access (OPC DA) was used to collect real-time sensor data from different sensors including UV, conductivity and LSPR. The LSPR sensor was operated by its own software on a separate computer so to avoid configuration issues the OPC DA data from the ÄKTA pure computer was tunnelled through Open Platform Communication United Architecture (OPC UA) using a Modelica model, developed in Wolfram System Modeler. A second Modelica model, running on the LSPR computer, was used to collect the real-time data from the two systems and present it in Wolfram System Modeler.

**2.4.3. Domain antibody (dAb) purification.** An ÄKTA pilot system was used for purification of dAb cell culture supernatants (dAb concentration: 1.4 mg mL<sup>-1</sup>) using a Capto™ L column 200 mL. The column was first equilibrated with 6 CV of 20 mM sodium citrate, 0.8 M NaCl, pH 5.0 at a flow rate of 163.6 mL min<sup>-1</sup>. After the sample was loaded, the column was washed using the equilibration buffer (5 CV) followed by another washing step using 20 mM sodium citrate, pH 5.0 (1 CV). Elution was done using 20 mM citrate buffer, pH 2.8. Washing and elution steps were carried out at a flow rate of 93.2 mL min<sup>-1</sup>. Protein G sensor chips were used for monitoring product breakthrough.

**2.4.4. Column leaking/breakthrough detection during mouse IgG2 and human IgG1 purification.** The samples were purified using an ÄKTA purifier system and using an in-house packed MabSelect SuRe 8 mL column at a flow rate of 3 mL min<sup>-1</sup>. Equilibration was performed using PBS. After sample loading, the column was washed until absorbance was below 50 mAU. 100 mM Glycine in PBS, pH 3.2 was used to elute IgG from the column. Protein A sensor chips were used for detection of product breakthrough and column leakage.

### 2.5. Off-line quantification of antibodies using LSPR

Quantification of antibodies was done using an HPLC pump and an injector connected to the LSPR flow cell. Protein A



sensor chips were inserted into the LSPR flow cell and equilibrated with phosphate buffered saline (PBS) pH 7.4 using a flow rate of  $1 \text{ mL min}^{-1}$ . Samples were manually injected into the flow cell through an injection valve, and sensor responses were recorded using the ArgusEye software. After each injection of samples, the sensor chip was regenerated using a one-minute pulse of  $10 \text{ mM}$  Glycine-HCl pH 2.5. All experiments were carried out at room temperature under ambient conditions. Binding responses after the sample injection ( $t = 200 \text{ s}$ ) were used for establishing a standard curve and for product quantification.

### 3. Results and discussion

#### 3.1. Real-time breakthrough curves of samples with different titers

To investigate the possibilities to use LSPR for specific detection of IgG in cell culture supernatants after the Protein A capture

steps we used samples with two different but known antibody concentrations;  $0.07$  and  $1.5 \text{ mg mL}^{-1}$ . During the loading phase, the presence of impurities in the effluent gave rise to significant UV background signals of approximately  $2920 \text{ mAU}$ . In contrast, the LSPR signals showed a negative base-line shift of about  $-2000 \text{ pm}$  due to the sample color (Fig. 2A and B). However, the base-line shift did not interfere with the IgG detection and can if needed be accounted for using a reference cell.

A significant increase in the LSPR response was seen when IgG broke through the column at  $\sim 88 \text{ min}$  and  $\sim 32 \text{ min}$  for the  $0.07 \text{ mg mL}^{-1}$  and  $1.5 \text{ mg mL}^{-1}$  samples, respectively. In contrast, because of the saturation of the UV detector due to background absorption, no signal increase was seen for the  $0.07 \text{ mg mL}^{-1}$  sample, and only a very minor increase for the sample with  $1.5 \text{ mg per mL}$  IgG. During the washing step, the LSPR baseline was restored and, with the addition of the bound IgG the response level reached  $1600 \text{ pm}$  (Fig. 2A) and  $2000 \text{ pm}$

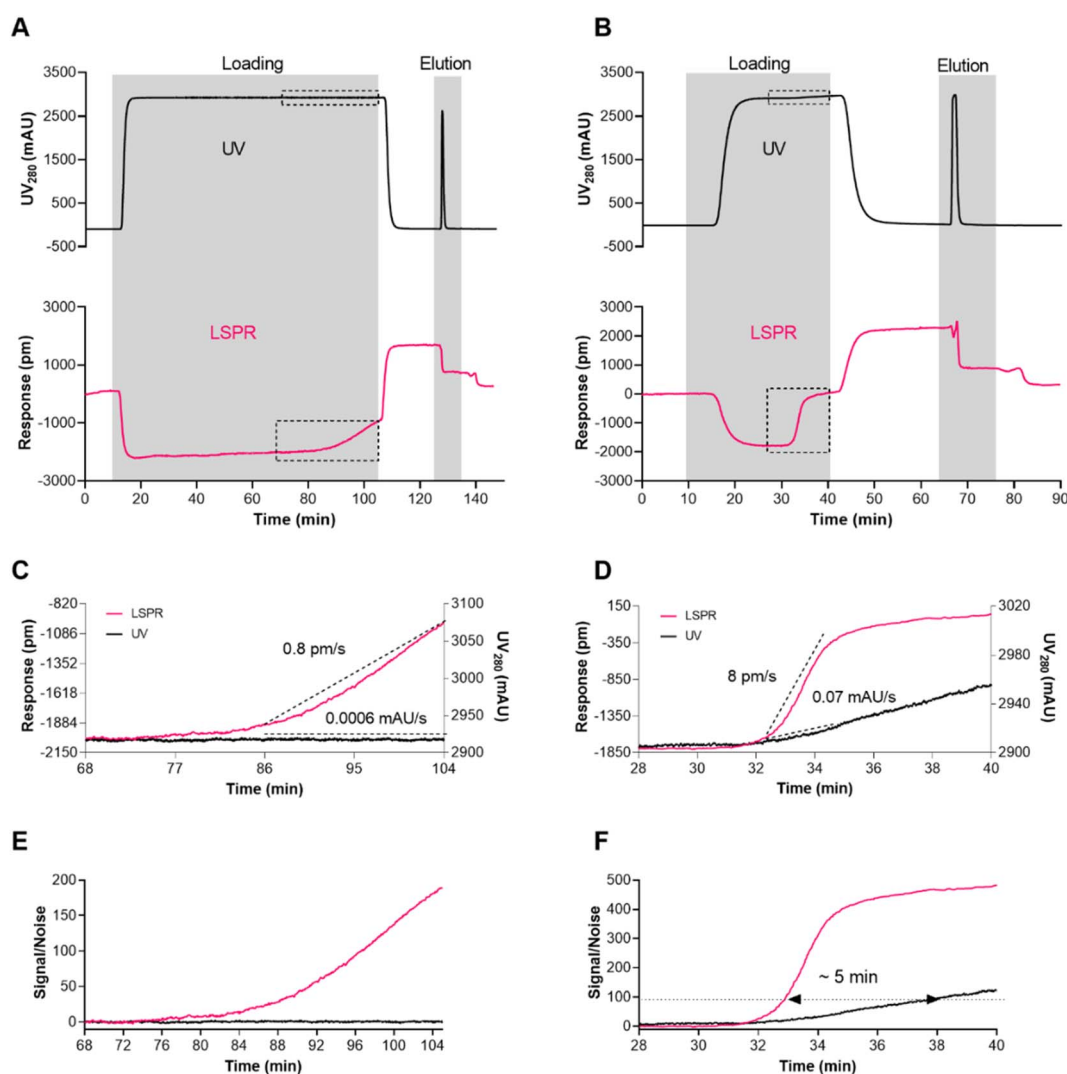


Fig. 2 (A) and (B) Real-time UV and LSPR signals from an IgG purification run using cell culture supernatant titers of  $0.07$  and  $1.5 \text{ mg mL}^{-1}$ , respectively. (C) and (D) UV and LSPR breakthrough curves corresponding to the dashed squares in (A) and (B), respectively. (E) and (F) Data from UV and LSPR breakthrough curves in (A) and (B), respectively, plotted as signal-to-noise, calculated from the raw UV and LSPR signals normalized to zero at  $68 \text{ min}$  (E) and  $28 \text{ min}$  (F) and thereafter divided by the averaged noise level of the baseline before the product breakthrough.





(Fig. 2B), for the two samples. When eluting IgG from the chromatography column using a pH 2.5 glycine buffer, the IgG bound to the sensor chips also dissociated, resulting in regeneration of the sensor chips. Therefore, the LSPR response returned to the initial baseline level at the end of the purification cycle. For samples containing 0.07 mg per mL IgG, the LSPR response increased with a mean slope of  $0.8 \text{ pm s}^{-1}$  starting from 86 min to 104 min, while the UV signals remained unchanged at 2920 mAU due to saturation of the detector (Fig. 2C). At the higher IgG concentration ( $1.5 \text{ mg mL}^{-1}$ ), the slope of the LSPR breakthrough curve was  $8 \text{ pm s}^{-1}$  (Fig. 2D) and was substantially more pronounced than the corresponding UV signal increase ( $0.07 \text{ mAU s}^{-1}$ ) (Fig. 2D).

Because the LSPR and UV detection have different units, the signal-to-noise ratio (S/N) for the respective data sets of the breakthrough curves were plotted for better comparison of the sensitivities of the two methods. The results showed significantly higher S/N values for the LSPR sensor system compared to conventional UV detection for both IgG concentrations (Fig. 2E and F). For the  $0.07 \text{ mg mL}^{-1}$  sample, while UV was not able to detect the IgG breakthrough, LSPR could detect this with a S/N value of about 200 (Fig. 2E). For the  $1.5 \text{ mg mL}^{-1}$  sample, the LSPR sensor showed a sharp increase in S/N from 26 to approximately 410 during breakthrough. In contrast, the S/N values obtained from UV were significantly lower than for the LSPR sensor even at the higher IgG concentration, with a moderate increase from 13 to 52. Therefore, LSPR provided product breakthrough detection significantly earlier than the UV sensor (Fig. 2F).

The observed dynamic binding capacity (DBC) for the  $1.5 \text{ mg mL}^{-1}$  sample was about 25 mg, which is close to the reported value (20 mg) by the column manufacturer. However, for the sample with the lowest concentration of IgG ( $0.07 \text{ mg mL}^{-1}$ ), the dynamic binding capacity was significantly reduced to only about 5 mg. This observation is well aligned with the typical behavior of Protein A columns where the DBC is decreased with lower sample concentrations, shorter residence times or higher flow rates.<sup>28</sup>

### 3.2. Breakthrough detection during multicycle purification

The LSPR sensor was further evaluated during a long ( $\sim 15 \text{ h}$ ) purification sequence comprising eight subsequent loading and elution cycles. The UV detector was saturated at about 3700 mAU and was not able to detect product breakthrough for any of the cycles (Fig. 3A and B). In contrast, the LSPR sensor detected product breakthrough in all eight purification cycles (Fig. 3C). The sensor surface was regenerated in-between each cycle during the stripping step. A small increase in the baseline level after each cycle indicated that the stripping step could be further optimized to ensure removal of more strongly bound species (e.g., product aggregates). The increasing baseline reduced the relative maximum sensor response over time (Fig. 3D), but this did not influence the breakthrough detection (Fig. 3E). In cycle 1, the product was observed to break through the column at 28.5 min, slightly earlier than in subsequent cycles with breakthrough points between 30 and 32.5 min

(Fig. 3F). This difference could be due to the fact that in the first cycle, the column was fresh and had not been exposed to the complex sample matrix. From cycle 2 to cycle 8, the column showed more consistent performance and had an average breakthrough time of 31 min. To determine the breakthrough time, noise levels over one minute, from 22 to 23 min, were extracted for each cycle and a mean value was calculated. The breakthrough time was defined as the point at which the relative response reached three times the noise level, corresponding to 28 pm. There was no significant changing in the breakthrough times over the purification cycles, indicating that the sensitivity for breakthrough detection was maintained over a multi-cycle run. The possibility to do repeated in-line product breakthrough detection using the LSPR sensor system with high sensitivity also in complex and strongly colored samples can facilitate the implementation of multicolumn chromatography and process intensification.

Time alignment is necessary to have an accurate comparison between LSPR responses and signals from UV and conductivity detectors in a chromatography run. The signals from the UV detector and LSPR sensor presented in Fig. 3A and C and conductivity signals (not shown) were collected using an open platform communication (OPC) solution. This OPC setup transferred the real-time signals for all three sensors into Wolfram System Modeler and enabled presenting all signals on a common time base to facilitate easy comparison. Also, having all the sensor signals in that system opens for further real-time signal processing and machine learning on the signals in the future.

To further explore the versatility and flexibility of the LSPR sensor system, we functionalized the sensor chips with Protein L for in-line breakthrough detection of antibody domain/fragments (dAb) (Fig. 4A). The affinity capture step was performed using a Protein L column connected to an ÄKTA pilot chromatography system with a flow rate set to  $93 \text{ mL min}^{-1}$ . Also, in this case it was impossible to detect the product in the effluent by UV due to the high background absorption, whereas a distinct increase in the LSPR signals could be observed upon product breakthrough (Fig. 4B). The results show both the potential of using LSPR for specific detection of different relevant molecular analytes by using suitable ligand-modified sensor chips and the possibilities to use the technique also for pilot purification scales under high flow rates. In addition, extending the flow rates up to  $200 \text{ mL min}^{-1}$  showed no negative effect to the performance of the LSPR sensor (Fig. S1, ESI†).

### 3.3. Detection of unexpected product leakage/breakthrough

We further evaluated the LSPR sensors in a routine affinity purification procedure at the R&D department of BioInvent AB, Lund, Sweden. UV and LSPR signals were recorded during purification of five different samples, including three mouse IgG2a (mIgG2a-01-03) and two human IgG1 (hIgG1-01-02), (Fig. 5A and B).

The amount of loaded sample was expected to be much lower than the column capacity; however, the LSPR sensor could detect some IgG leaking out of the column at about 90–110 min



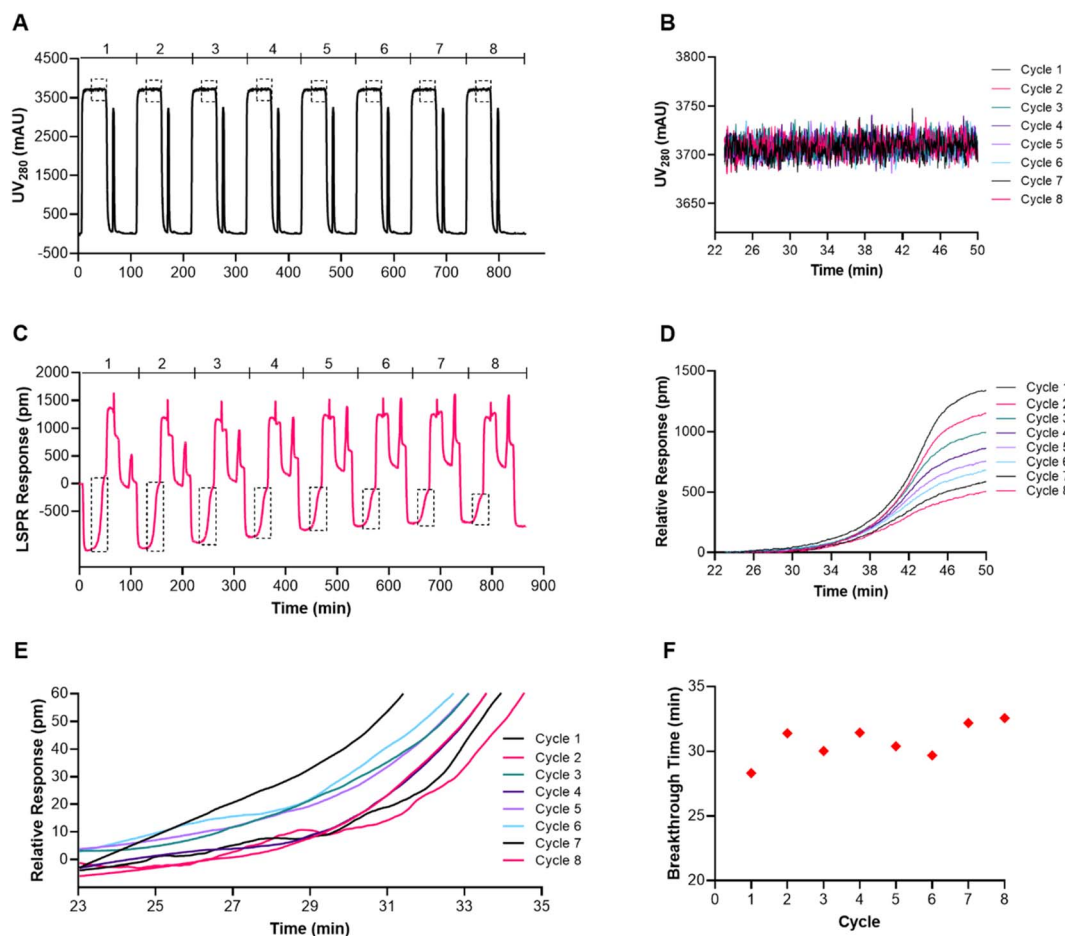


**Fig. 3** (A) UV signals from eight subsequent cycles of IgG purification. Dashed rectangles mark the time range where product breakthrough was expected. (B) Zoomed-in UV signals from 23 to 50 min. (C) LSPR signals from eight subsequent cycles of IgG purification. Dashed rectangles mark the time range where product breakthrough was observed. (D) Breakthrough curves from eight cycles. The relative binding responses are the difference between the absolute responses and the baseline at 23 min of each cycle before the breakthrough occurs. (E) Zoomed-in area (from 23 to 35 min) of noise-reduced breakthrough curves. (F) Breakthrough time of each cycle. Breakthrough time was defined as breakthrough points at which relative responses reach three times the noise or Limit of Detection (LOD), corresponding to 28 pm.

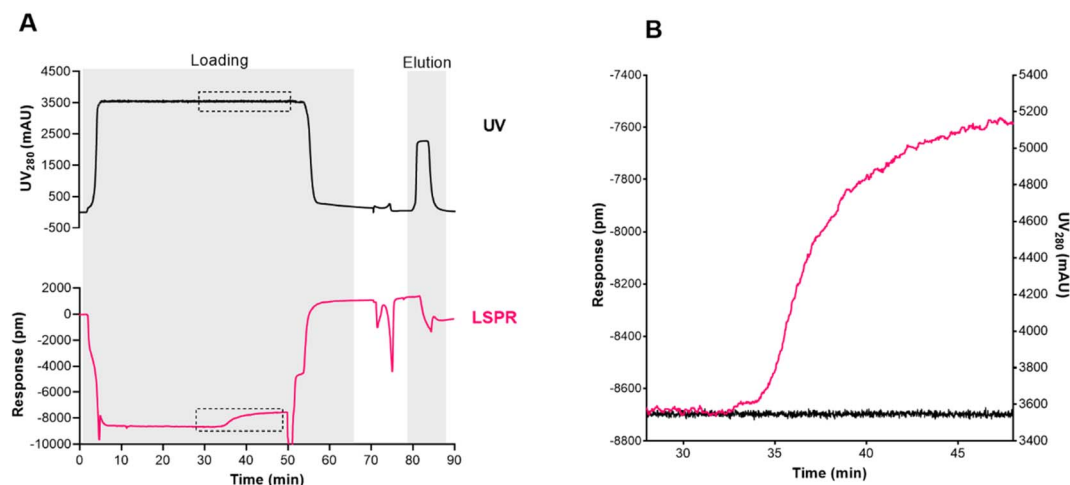


**Fig. 4** (A) UV (black) and LSPR (red) signals from a dAb purification step in an ÄKTA pilot system. (B) Breakthrough curves from the timespan indicated by the dashed squares in A.



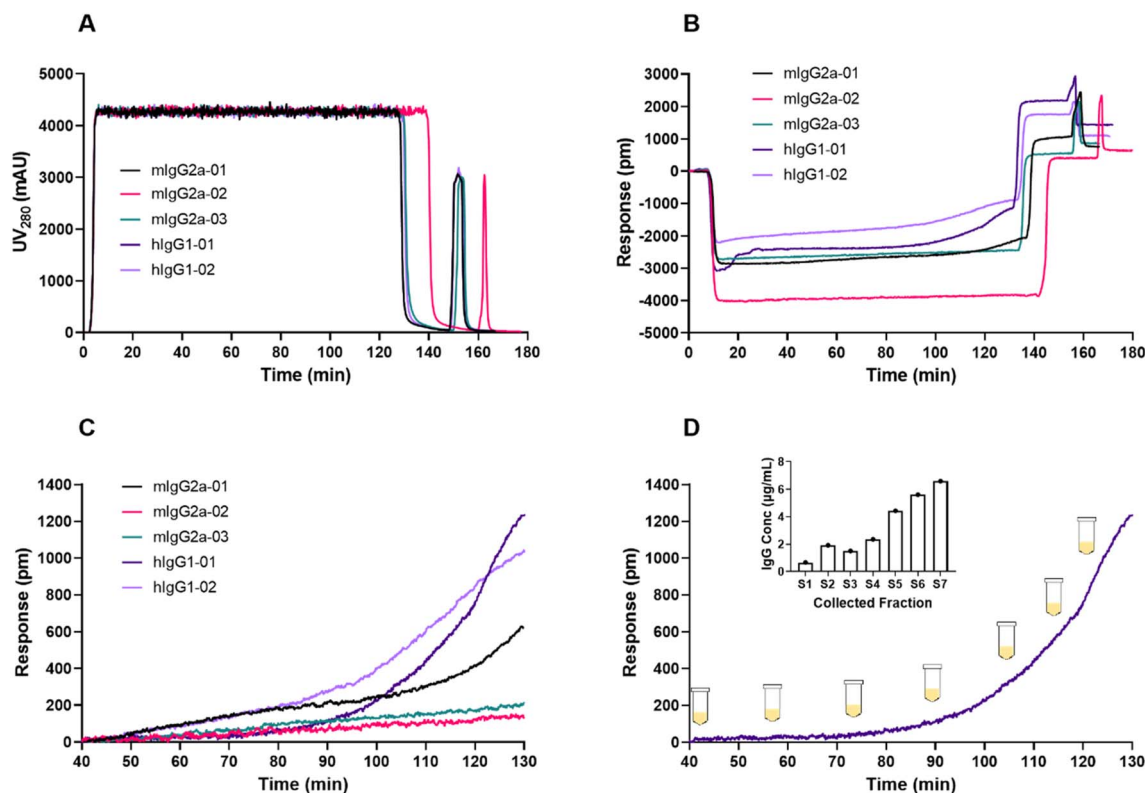


Fig. 5 (A) Overlaid UV signals and (B) LSPR responses in affinity purification of three mouse IgG2a samples, mlgG2a\_01 ( $0.19 \text{ mg mL}^{-1}$ ), mlgG2a\_02 ( $0.02 \text{ mg mL}^{-1}$ ) and mlgG2a\_03 ( $0.16 \text{ mg mL}^{-1}$ ) and two human IgG1 samples, hlgG1\_01 ( $0.28 \text{ mg mL}^{-1}$ ) and hlgG1\_02 ( $0.3 \text{ mg mL}^{-1}$ ). Chromatography runs were performed using an ÄKTA Explore system with a flow rate of  $3 \text{ mL min}^{-1}$  using elution pH of 2.8. (C) Relative LSPR responses of five samples baseline-adjusted to zero at 40 min. (D) Breakthrough curve of the hlgG1\_01 sample and determined concentrations of seven fractions collected at different time points at the end of the loading phase.

for three out of five different IgG samples tested (Fig. 5B and C). In contrast, the UV detector was saturated during the loading phase (Fig. 5A) and was not able to detect the IgG in the effluent. It was noticed that there was a correlation between concentrations and time points for the observed column leakage for the five samples. No leakage was observed for mlgG2a\_02 ( $\sim 0.02 \text{ mg mL}^{-1}$  IgG) and mlgG2a\_03 ( $\sim 0.16 \text{ mg mL}^{-1}$  IgG), which had lower concentrations compared to the other three samples. Among the three samples in which the LSPR sensor system could detect column leakage, samples hlgG1\_01 ( $\sim 0.3 \text{ mg mL}^{-1}$ ) and hlgG1\_02 ( $\sim 0.3 \text{ mg mL}^{-1}$ ) had higher concentrations than mlgG2a\_01 ( $\sim 0.19 \text{ mg mL}^{-1}$ ) and were found to leak from the column at an earlier timepoint (Fig. 5C). This observation is reasonable considering that both human IgG1 and mouse IgG2a have strong and almost equal binding strength to Protein A.<sup>29</sup>

Seven fractions were collected during the loading cycle when the breakthrough was observed, starting from 40 min to 130 min for the hlgG1\_01 sample ( $\sim 0.3 \text{ mg mL}^{-1}$ ) (Fig. 5D). Off-line IgG quantification (Fig. S2, ESI†) of these fractions using LSPR showed an increase in the IgG concentrations from approximately  $0.2 \text{ μg mL}^{-1}$  to  $7 \text{ μg mL}^{-1}$ , confirming the leakage/breakthrough of IgG after 80 min. The selectivity and

sensitivity of the LSPR sensor system were consistent with previous results.<sup>25</sup>

## 4. Conclusions

We have demonstrated a novel real-time in-line sensor technique based on LSPR for detection of product breakthrough and column leakage during the loading phase in affinity capture steps. Due to the high selectivity of the sensor chips and the high affinity for binding of target analytes, the LSPR sensor provides sensitive detection of specific protein-based products in the effluent containing a significant amount of non-product related proteins and impurities. The sensor enabled in-line detection of IgG at concentrations as low as  $2 \text{ μg mL}^{-1}$  in complex cell culture harvest matrices whereas the UV sensor was saturated due to high background absorption. The LSPR sensor thus enables early and sensitive detection of product breakthrough and column leakage which can minimize loss of precious samples. Moreover, the possibility to regenerate the sensor surface in-line during the column stripping step enabled reuse of the sensor for multiple purification cycles, with retained sensitivity for detection of product breakthrough during eight continuous cycles over a period of 15 hours. The possibilities to functionalize the sensor chips with different



ligands was further demonstrated for in-line detection of dAb. In addition, the sensor system is very robust and could be used at different purification scales. This LSPR sensor technology can consequently dramatically improve capabilities for in-line product monitoring during capture steps and facilitate development of automated processing, multicolumn chromatography and continuous bioprocessing.

## Conflicts of interest

D. A., E. M., I. L., and C. F. M. are cofounders and shareholders of ArgusEye AB.

## Acknowledgements

Funding from the European Union's Horizon 2020 research and innovation program under the Marie Skłodowska-Curie grant agreement No. 841373 and the Swedish Innovation Agency (VINNOVA), grant numbers 2016-04120 and 2019-00130, are gratefully acknowledged. We are very thankful to the staff at Testa Center, Uppsala, Sweden for their assistance with the chromatography measurements at the Testa Challenge 2020 and 2022.

## References

- 1 F. C. Breedveld, *Lancet*, 2000, **355**, 735–740.
- 2 R.-M. Lu, Y.-C. Hwang, I. J. Liu, C.-C. Lee, H.-Z. Tsai, H.-J. Li and H.-C. Wu, *J. Biomed. Sci.*, 2020, **27**, 1.
- 3 A. Matte, *Int. J. Mol. Sci.*, 2022, **23**, 8663.
- 4 S. Hober, K. Nord and M. Linhult, *J. Chromatogr. B: Anal. Technol. Biomed. Life Sci.*, 2007, **848**, 40–47.
- 5 A. A. Shukla, B. Hubbard, T. Tressel, S. Guhan and D. Low, *J. Chromatogr. B: Anal. Technol. Biomed. Life Sci.*, 2007, **848**, 28–39.
- 6 S. Kanje, J. Scheffel, J. Nilvebrant and S. Hober, in *Approaches to the Purification, Analysis and Characterization of Antibody-Based Therapeutics*, ed. A. Matte, Elsevier, 2020, ch. 2, pp. 35–54.
- 7 G. R. Bolton and K. K. Mehta, *Biotechnol. Prog.*, 2016, **32**, 1193–1202.
- 8 A. M. Ramos-de-la-Peña, J. González-Valdez and O. Aguilar, *J. Sep. Sci.*, 2019, **42**, 1816–1827.
- 9 P. Gronemeyer, R. Ditz and J. Strube, *Bioengineering*, 2014, **1**, 188–212.
- 10 C. Murphy, T. Devine and R. O'Kennedy, *Antib. Technol. J.*, 2016, **6**, 17–32.
- 11 D. Baur, M. Angarita, T. Müller-Späth, F. Steinebach and M. Morbidelli, *Biotechnol. J.*, 2016, **11**, 920–931.
- 12 D. Baur, J. M. Angelo, S. Chollangi, X. Xu, T. Müller-Späth, N. Zhang, S. Ghose, Z. J. Li and M. Morbidelli, *J. Biotech.*, 2018, **285**, 64–73.
- 13 J. Guo, M. Jin and D. Kanani, *Biotechnol. J.*, 2020, **15**, 2000192.
- 14 F. Steinebach, N. Ulmer, M. Wolf, L. Decker, V. Schneider, R. Wälchli, D. Karst, J. Souquet and M. Morbidelli, *Biotechnol. Prog.*, 2017, **33**, 1303–1313.
- 15 R. Godawat, K. Konstantinov, M. Rohani and V. Warikoo, *J. Biotechnol.*, 2015, **213**, 13–19.
- 16 R. E. Mushens, A. R. Guest and M. L. Scott, *J. Immunol. Methods*, 1993, **162**, 77–83.
- 17 J. Horak, A. Ronacher and W. Lindner, *J. Chromatogr. A*, 2010, **1217**, 5092–5102.
- 18 L. Paradina Fernandez, L. Calvo and L. Vina, *Int. Scholarly Res. Not.*, 2014, **2014**, 487101.
- 19 Cytiva, *Lifetime performance study of MabSelect Prisma during repeated cleaning-in-place cycles*, <https://cdn.cytivalifesciences.com/dmm3bwsv3/AssetStream.aspx?mediaformatid=10061&destinationid=10016&assetid=26523>, accessed 20/09/2022.
- 20 J. Zhang, S. Siva, R. Caple, S. Ghose and R. Gronke, *Biotechnol. Prog.*, 2017, **33**, 708–715.
- 21 F. Feidl, M. F. Luna, M. Podobnik, S. Vogg, J. Angelo, K. Potter, E. Wiggin, X. Xu, S. Ghose, Z. J. Li, M. Morbidelli and A. Butté, *J. Chromatogr. A*, 2020, **1625**, 461261.
- 22 P. Bångtsson, E. Erik, K. Lacki and H. Skoglar, WO2010151214A1, 2010.
- 23 R. Godawat, K. Brower, S. Jain, K. Konstantinov, F. Riske and V. Warikoo, *Biotechnol. J.*, 2012, **7**, 1496–1508.
- 24 R. A. Chmielowski, L. Mathiasson, H. Blom, D. Go, H. Ehring, H. Khan, H. Li, C. Cutler, K. Lacki, N. Tugcu and D. Roush, *J. Chromatogr. A*, 2017, **1526**, 58–69.
- 25 T. Tran, O. Eskilson, F. Mayer, R. Gustavsson, R. Selegård, I. Lundström, C.-F. Mandenius, E. Martinsson and D. Aili, *Processes*, 2020, **8**, 1302.
- 26 M. Kisovec, G. Anderluh, M. Podobnik and S. Caserman, *Anal. Biochem.*, 2020, **608**, 113899.
- 27 G. Thakur, V. Hebber and A. S. Rathore, *Biotechnol. Bioeng.*, 2020, **117**, 673–686.
- 28 E. Müller and J. Vajda, *J. Chromatogr. B: Anal. Technol. Biomed. Life Sci.*, 2016, **1021**, 159–168.
- 29 Cytiva, *Affinity Chromatography vol. 1, Antibodies*, <https://cdn.cytivalifesciences.com/api/public/content/digi-11660-pdf>, accessed 20/09/2022.

